

New Insights into the Mechanism of Reduction of Tertiary Phosphine Oxides by Means of Phenylsilane

Oleg M. Demchuk,¹ Radomir Jasiński,² and K. Michał Pietrusiewicz¹

¹Department of Organic Chemistry, Maria Curie-Skłodowska University, Lublin 20614, Poland

²Institute of Organic Chemistry and Technology, Cracow University of Technology, Cracow 31155, Poland

Received 30 March 2015; revised 16 June 2015

ABSTRACT: *The mechanism of the reduction of phosphine oxides by PhSiH₃ was established on the basis of kinetic measurements and Density Functional Theory (DFT) calculations. In particular, it has been proved that the model reaction between tri-*n*-butylphosphine oxide and phenylsilane occurs via a nonpolar mechanism. The data presented herein allow prediction and verification of the applicability of the new reduction reagents and conditions for industrially attractive processes.* © 2015 Wiley Periodicals, Inc. Heteroatom Chem. 26:441–448, 2015; View this article online at wileyonlinelibrary.com. DOI 10.1002/hc.21279

INTRODUCTION

Phosphines constitute an important class of organic compounds with well-recognized academic and industrial usage as ligands, organocatalysts, extractants, etc. [1]. The main approach to phosphines remains reduction of phosphine oxides by various strong reducing agents. Numerous research groups have studied such reductions as well as the applicability of different reductants. In terms of reaction yields and selectivity, the most promising reducing agents include silanes [2], Si₂Cl₆ [3], HSiCl₃/Et₃N [4], HSiCl₃/Ph₃P [5],

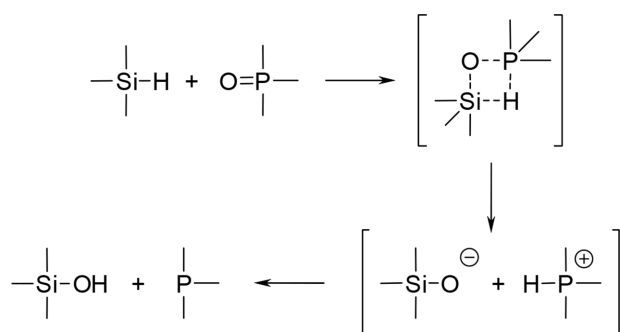
Ti(OiPr)₄/HSi(OEt)₃ [6–8], Ti(OiPr)₄/PMHS [9, 10], TMDS/Cu(OTf)₂ [11], (EtO)₂MeSiH/Ar₂PO₂H [12], PhSiH₃ [13, 14], LiAlH₄ [15, 16], LiAlH₄/MeOTf [17], AlH₃ [18, 19], DIBAL-H [20], and Schwartz reagent [Cp₂ZrHCL] [21]. Nevertheless, the utilization of majority of frequently used reductants suffers from their toxicity, corrosiveness, low stereoselectivity, and the necessity to use expensive additives, or unfavorable conditions.

Considerably less demanding and therefore more commonly used is the reduction of phosphine oxides by phenylsilanes [13]. They offer considerable advantages over other reducing agents [2], such as nonaggressive behavior, simple and mild reaction conditions, low toxicity, good functional group tolerance, relatively simple purification of products, and a predictable and highly enantioselective stereochemical outcome. For these advantages, they have been recently used as suitable reductants in the key steps of catalytic Wittig [22–24], Appel [25], Mitsunobu [26–28], as well as in related reactions [29]. Thus, investigation of the precise mechanism of reduction of phosphine oxides by phenylsilane has an additional practical value since it can help to develop new reagent systems for those industrially attractive processes.

Despite the potentially high value of such studies, the publications dedicated to elucidation of the mechanism of deoxygenation of phosphine oxides are very rare and not comprehensive. The mechanism of reduction of phosphine oxides by chlorosilane had been initially proposed by Horner and

Correspondence to: Oleg M. Demchuk; e-mail: oledemchuk@umcs.lublin.pl

© 2015 Wiley Periodicals, Inc.



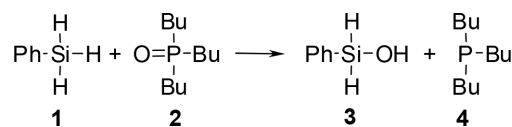
SCHEME 1 Hypothetical ionic mechanism for the reaction between tertiary phosphine P-oxides and phenylsilane [13].

Balzer [4]. More detailed results of theoretical studies of the mechanism of reduction of phosphine oxides by trichlorosilane have been presented only recently by Krenske [30]. Based on this purely theoretical investigation run by means of DFT and Møller–Plesset calculations, Krenske found that the reaction runs through two different mechanisms leading to products with inversion or retention of absolute configuration at the phosphorus atom, depending on the reaction conditions and reagent systems. For analogous reductions of phosphine oxides by phenylsilane, an intuitive polar, two-step mechanism involving formation of an ion-pair intermediate (Scheme 1) was proposed by Marsi [13], but it has not been so far verified in any way.

In respect to the crucial importance of phenylsilane-based reduction of phosphine oxides, we aimed to study the mechanism of this reaction both experimentally and theoretically, using tri-*n*-butylphosphine oxide (**2**) and phenylsilane (**1**) as model reactants.

RESULTS AND DISCUSSION

Among the number of available phosphine oxides, tri-*n*-butylphosphine oxide (**2**) was selected as a model reactant because of its low hygroscopicity (experimental kinetic results not influenced by water impurities), high solubility in numerous organic solvents, and a moderate reduction reaction rate observed in preliminary experiments. Besides their applicability in the DFT calculations, cyclic phosphine oxides and those bearing smaller substituents (Me, Et, Pr) at the phosphorus atom were highly hygroscopic, while the tested aromatic derivatives were insoluble in nonpolar solvents. It was found that an increase in sterical hindrance at the phosphorus atom slowed down the reaction significantly; therefore, the use of bulky oxides was also limited. (Scheme 2).



SCHEME 2 Reduction of **2** by means of phenylsilane (**1**).

TABLE 1 Representative Conditions for the Reaction between Tri-*n*-butylphosphine oxide (**2**) and Phenylsilane (**1**)

Entry	Solvent	Ratio (1):(2)	Time (h)	<i>t</i> (°C)	Conv.(2) (%)
1	PhSiH ₃	80:1	4	100	95
2	PhSiH ₃	80:1	4	75	39
3	PhSiH ₃	80:1	17	75	97
4	PhSiH ₃	80:1	90	50	99
5	C ₆ H ₁₂	20:1	5	75	47
6	DME	20:1	5	75	10
7	DMSO	20:1	5	75	10
8	CPME	20:1	32	75	98

To assure reliable results, all kinetic experiments were conducted in sealed vessels and the reaction mixtures were always protected by argon atmosphere in sealed reactors to exclude possible oxidation and evaporation effects, which may influence the quantitative results. The extent of substrate conversions was monitored by means of ³¹P, ¹H, and ¹³C NMR spectroscopy of rapidly cooled samples. It was found that in reactions where phenylsilane was used both as the solvent and the reactant, full conversion of **2** was observed in 4 h at 100°C and in 90 h at 50°C. Having these promising results, series of experiments were carried out in different solvents, with different reagent ratios, and at different temperatures (Table 1). The reactions were run at temperatures between 50 and 100°C, since preliminary experiments run at room temperature (RT) took several weeks to achieve sufficient conversion, and reactions run above 100°C were too short to perform kinetic experiments with good precision.

In the detailed investigation of the reaction course, intermolecular interactions in the elementary reaction process with respect to the recently widely promoted [31, 32] theory of global electrophilicity and nucleophilicity indexes were analyzed first. Recently, the approach based—according to the Domingo suggestions [31]—on B3LYP/6-31G(d) calculations has been used successfully for the interpretation of different bimolecular reactions [31–35]. Indices necessary for this purpose (chemical electron potentials μ , chemical hardness η , global electrophilicity ω , as well as maximum charge that may be potentially accepted in the electrophilic substructure of transition complex ΔN_{\max}) were

TABLE 2 Global Electronic Properties for Phenylsilane (**1**) and Tri-*n*-butylphosphine oxide (**2**)

Compound	μ (a.u.)	η (a.u.)	ω (eV)
1	-0.1347	0.2343	1.05
2	-0.1108	0.2018	0.83

calculated as a function of Frontier Molecular Orbitals (FMO) energies (Table 2).

The analysis of chemical electron potentials proved that the electron transfer in the reaction should occur from oxide **2** ($\mu = -0.1108$ a.u.) to phenylsilane **1** ($\mu = -0.1347$ a.u.). The maximum charge potentially accepted by the phenylsilane molecule within the transition complex (ΔN_{\max}) is almost 0.6 eV. Both reaction components are considered moderate electrophiles [31], where phenylsilane global electrophilicity is slightly higher. The difference between global electrophilicity values for the substrates is not large ($\Delta\omega = 0.22$ eV). Therefore, the reaction should be considered a nonpolar process.

The character of the interactions in the first reaction stage is evaluated based on electronic properties. Its mechanism, however, cannot be analyzed in this way. Therefore, to describe precisely the nature of critical structures on the substrate conversion pathway toward the products, we simulated the reaction pathway based on the DFT calculations data. The calculations were made in several basis sets using the B3LYP functional [36], successfully verified

for a number of organophosphorus compounds, including phosphines and their oxides [37] and, additionally, using a new generation M062x functional [38]. For the calculations of the solvent effect on the reaction paths, the polarizable continuum model (PCM) was used.

The results of B3LYP/6-31g(d) (PCM) simulations prove that the reaction between tri-*n*-butylphosphine oxide (**2**) and phenylsilane (**1**) is a multistage process. In particular, two transition complexes (**TS-1** and **TS-2**) were localized between the minimum linked with existence of individual substrates (**1** + **2**) and the minimum linked with existence of products (**3** + **4**) separated by the intermediate minimum (**I**) and a minimum corresponding to the prereaction complex (PC) (Tables 3 and 4). The shape of the enthalpic reaction profile is shown in Fig. 1, and the visualisations of the critical structures are shown in Fig. 2.

Interactions between the reagent molecules in the first stage lead to the formation of PC. This involves the enthalpy of the reaction system reduced by 1.7 kcal/mol. The complex has no properties of a charge transfer one. Distances between the reaction centers in the complex are still much larger than the range typical of respective transition state bonds.

Further movement of the reaction system along the reaction coordinate lead to the formation of intermediate **TS-1**. This involves an increase in the enthalpy of the reaction system by 28.5 kcal/mol. This is the limiting step for the whole process. With the increased enthalpy,

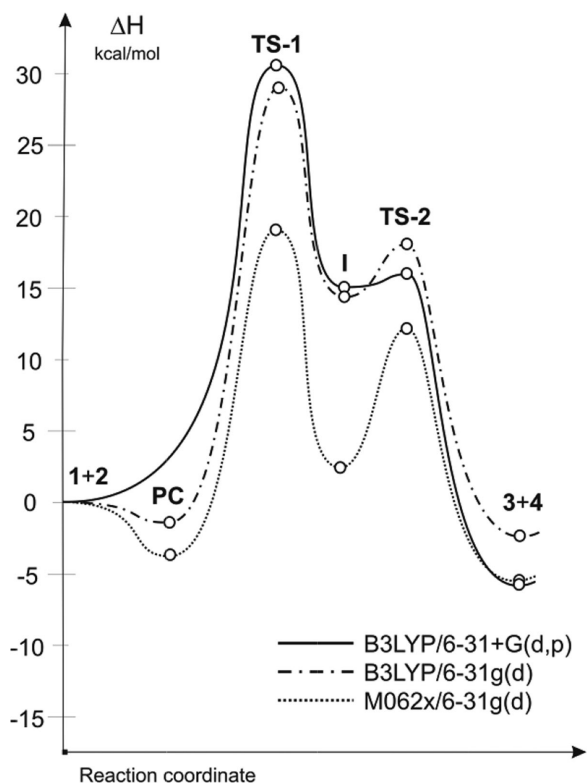
TABLE 3 Eyring Parameters of the Reaction between Phenylsilane (**1**) and Tri-*n*-butylphosphine oxide (**2**) in Solution according to DFT (PCM) Calculations

Basis set	Transition	Functional					
		B3LYP			M062x		
		ΔH	ΔG	ΔS	ΔH	ΔG	ΔS
6-31G(d)	1 + 2 \rightarrow PC	-1.7	7.55	-31.1	-4.0	3.55	-25.2
	1 + 2 \rightarrow TS-1	28.5	43.06	-48.9	18.7	30.95	-41.0
	1 + 2 \rightarrow I	14.0	26.70	-42.6	2.6	15.72	-43.9
	1 + 2 \rightarrow TS-2	18.2	30.33	-40.9	12.0	25.36	-44.7
	1 + 2 \rightarrow 3 + 4	-2.5	-2.59	0.2	-5.7	-6.40	2.4
6-31+G(d)	1 + 2 \rightarrow PC	-0.1	7.57	-25.8	-3.0	4.35	-24.6
	1 + 2 \rightarrow TS-1	31.0	45.64	-49.0	20.3	33.34	-43.6
	1 + 2 \rightarrow I	15.3	27.61	-41.4	2.9	18.14	-51.0
	1 + 2 \rightarrow TS-2	17.1	27.92	-36.3	10.7	22.59	-40.0
	1 + 2 \rightarrow 3 + 4	-3.1	-2.87	-0.8	-6.4	-7.11	2.4
6-31+G(d,p)	1 + 2 \rightarrow PC				-3.1	4.96	-27.2
	1 + 2 \rightarrow TS-1	30.8	45.23	-48.4	20.2	33.05	-43.1
	1 + 2 \rightarrow I	15.0	27.33	-41.4	2.6	17.75	-50.9
	1 + 2 \rightarrow TS-2	16.3	27.77	-38.4	4.8	16.03	-37.6
	1 + 2 \rightarrow 3 + 4	-6.0	-5.75	-0.9	-9.2	-9.90	2.3

ΔH and ΔG values are expressed in kcal/mol; ΔS values are expressed in cal/mol·K.

TABLE 4 Key Geometrical Parameters of Critical Structures **PC**, **TS-1**, **I**, and **TS-2** in Solution according to B3LYP/6-31g(d) (PCM) Calculations

Structure	Interatomic Distances r (Å)					Degree of Bond Development		
	Si-H	H-P	P-O	O-Si	H-O	H-P	Si-O	O-H
PC	1.488	4.622	1.515	3.730	3.439			
TS-1	1.708	1.934	1.617	1.786	2.167	0.629	0.903	
I	2.894	1.411	1.936	1.628	2.252			
TS-2	3.255	1.412	2.767	1.600	1.853			0.087

**FIGURE 1** Enthalpy profile of the reaction between phenylsilane (**1**) and tri-*n*-butylphosphine oxide (**2**) according to calculations at selected DFT (PCM) levels.

entropy of the reaction system is reduced by 48.9 cal/mol·K. This suggests that **TS-1** is highly rigid. Indeed, a detailed geometry analysis proved the structure to be a four-membered complex, at the first view similar to that postulated by Marsi [13]. However, its nature is different from that suggested by the authors. In particular, two new σ -bonds form within **TS-1**. They are silicon–oxygen and hydrogen–phosphorus bonds. The degrees of their advancement were estimated based on the relationship (Eq. (1)):

$$l_{X-Y} = 1 - \frac{r_{X-Y}^{\text{TS}} - r_{X-Y}^{\text{P}}}{r_{X-Y}^{\text{P}}} \quad (1)$$

where r_{X-Y}^{TS} is the distance between the reaction centers X and Y at the transition structure and r_{X-Y}^{P} is the same distance at the corresponding product.

The complex proved to be nonsymmetrical. The Si–O ($r = 1.786$ Å, $l = 0.903$) bond forms much more rapidly. The Si–H bond is broken when the new σ -bonds form. Further development of the reaction system lead to the formation of intermediate **I**. Contrary to what Marsi [13] suggested, this is not an ion pair. In the intermediate, the Si–O bond is already formed ($r = 1.628$ Å). The O–P distance is also typical of the formed chemical bond. It should be noted at this point that the presence of a similar phosphorane intermediate has been suggested by Mislow and co-workers [3] in the case of reduction of optically active acyclic phosphine oxides by means of hexachlorodisilane. Intermediate **I** is unstable, rapidly converted further through the transition state **TS-2**. **TS-2** formation involves a relatively lower energy expense than for **TS-1**. It is a three-membered complex. An O–H bond forms within its structure. The degree of advancement of the bond in **TS-2** does not exceed 10%, however. P–O and H–P bonds are simultaneously broken. Similar transformation has been previously studied both experimentally and theoretically [39]. Further movement of the reaction system leads to the products (**3 + 4**). To conclude, the reaction mechanism is shown in Scheme 3.

DFT calculation data at other theory levels (Tables 3 and 4) provide a similar profile of the reaction. In particular, energy profiles are very similar and the geometry parameters of critical structures are practically identical as for the B3LYP/6-31G(d) calculations. This changes only qualitative description of critical points in the enthalpic profiles. All attempts to find ionic intermediates as well as hypothetical one-step reaction paths (including calculations in more advanced 6-31+G(d) and 6-31+G(d,p) basis sets) were not successful.

Next, we performed similar calculations for the reaction in the gas phase. It was found (Table 5) that the reaction mechanism is practically identical as in the presence of a dielectric medium. It was further

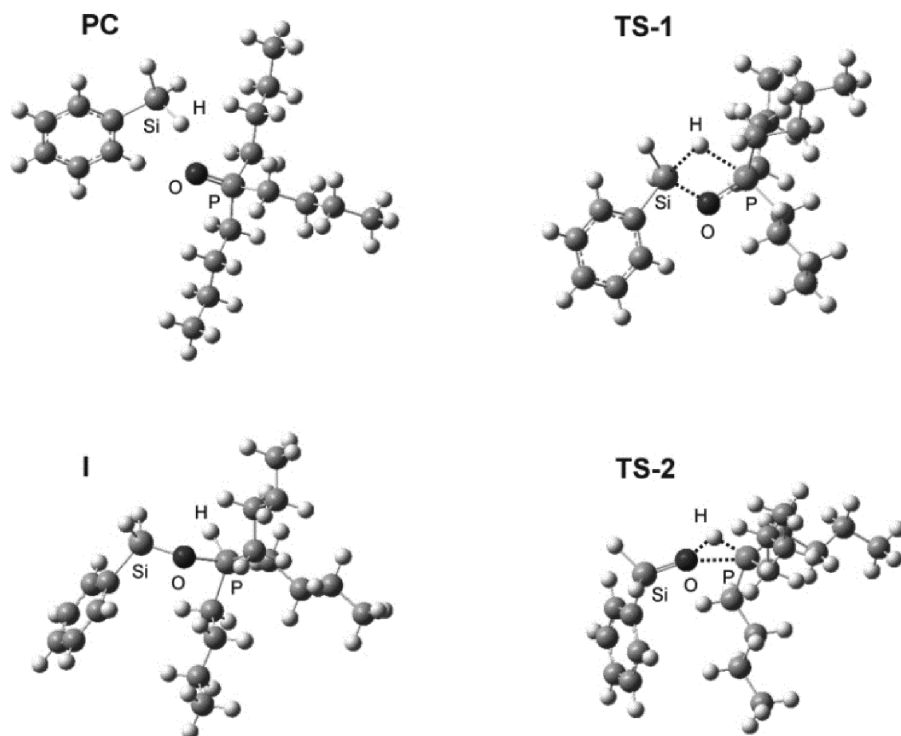
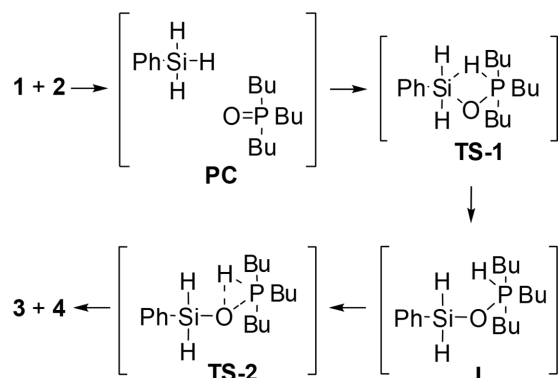


FIGURE 2 Critical structures of the reaction between phenylsilane (1) and tri-*n*-butylphosphine P-oxide (2) according to B3LYP/6-31G(d) (PCM) calculations.



SCHEME 3 Mechanism of the reaction between phenylsilane and tertiary phosphine P-oxides according to the DFT calculations.

confirmed that the reaction between **1** and **2** has a nonionic character.

To determine which theory level is better in describing the energetic aspects of reaction course, we decided to establish activation enthalpy and entropy values under experimental conditions. Therefore, measurements of rate constants at three temperatures were performed (Table 6) and the Eyring relationship was determined (Eq. (2)) [40].

$$\log(k/T) = 10.319 + \Delta S^\ddagger/4.576 - \Delta H^\ddagger/4.576T \quad (2)$$

The resulting activation enthalpy was 17.02 kcal/mol, while the activation entropy

TABLE 5 Eyring Parameters of the Reaction between Phenylsilane (1) and Tri-*n*-butylphosphine oxide (2) in the Gas Phase according to DFT Calculations

Transition	B3LYP/6-31G(d)		B3LYP/6-31+G(d)		B3LYP/6-31+G(d,p)		M062x/6-31g(d)	
	ΔH	ΔS	ΔH	ΔS	ΔH	ΔS	ΔH	ΔS
1+2 → PC	-2.7	-30.0	-1.6	-26.8	-1.6	-26.9	-9.7	-30.4
1+2 → TS-1	27.6	-48.6	29.5	-48.6	29.4	-48.6	18.8	-34.6
1+2 → I	11.6	-41.6	12.5	-42.0	12.2	-42.0	-0.2	-47.5
1+2 → TS-2	19.7	-40.5	18.6	-37.3	17.7	-37.8	14.0	-33.2
1+2 → 3+4	-3.8	0.6	-4.9	-0.8	-7.9	-1.0	-6.4	6.5

ΔH values are expressed in kcal/mol; ΔS values are expressed in cal/mol·K.

TABLE 6 Experimental Measured Rate Constants of the Reaction between Phenylsilane (**1**) and Tri-*n*-butylphosphine oxide (**2**)

Entry	<i>t</i> (°C)	<i>k</i> × 10 ⁻⁶ (1/mol·s)
1	50	1.16
2	75	8.47
3	100	46.81

was 33.2 cal/mol·K. The values satisfactorily correlate with the M062x/6-31g(d) (PCM) calculations. The relatively low activation enthalpy value confirms that the energy changes in the reacting system caused by breaking the existing σ -bonds are compensated by changes related to the formation of new bonds. Furthermore, the high negative activation entropy confirms that **TS-1** is highly ordered.

Finally, it has to be noted that despite the fact of the different reactivity of chlorosilane and phenylsilane, our comprehensive (theoretical and experimental) results correlate well with the previous, only theoretical study presented by Krenske [30]. Therefore, this may suggest a general character of the described transformation and that the proposed mechanism can be extrapolated to reactions involving different classes of silicon-based reductants such as several phosphine oxides. This is confirmed additionally by our calculations of the reaction paths for reductions of other tertiary phosphine oxides by means of several arylsilanes. All of these reactions proceed via an identical, two-step mechanism, as in the case of tri-*n*-butylphosphine oxide reduction. It should also be mentioned that 1-phenylphospholane oxide is converted into 1-phenylphospholane via an activation barrier, which is a few kcal/mol lower than in the case of similar reduction involving tri-*n*-butylphosphine oxide. This observation correlated well with the recent results from the Krenske group [41]. Our experiments also show that a similar kinetic effect stimulates electron withdrawing groups in the phenyl ring of silane [22].

CONCLUSIONS

The theoretical and experimental studies provide new insights into the mechanism of reactions between tertiary phosphine oxides and silanes. In particular, it has been proved that the model reaction between tri-*n*-butylphosphine oxide and phenylsilane occurs via a nonionic mechanism. The first stage involves the formation of a PC which, subsequently, is converted to the intermediate through the first transition complex. Further development

of the reaction leads to conversion of the intermediate to phenylsilanol and tri-*n*-butylphosphine through a three-membered transition complex. All attempts to find an alternative mechanism for tri-*n*-butylphosphine reduction were—irrespective of the theory level—not successful. The results obtained in our investigations allow prediction and verification (by DFT calculation according to the proposed algorithm) of the applicability of the new reduction reagents and conditions for industrially attractive processes.

EXPERIMENTAL

Materials and Equipment

The reactions were carried out under dry argon atmosphere. Unless noted otherwise, materials were obtained from commercial suppliers and used as received. Thin layer chromatography was performed on Merck silica gel 60 coated aluminum plates. NMR spectra were recorded on a Bruker Advance III spectrometer (500 MHz at ¹H NMR). All commercially available reagents and solvents were purchased from Sigma-Aldrich and used without further purification. Tetramethylsilane, deuterium oxide (in a sealed capillary), or phosphoric acid (75% in a sealed capillary) were used as internal standards. All NMR spectra were reported in delta (δ) units, parts per million (ppm) downfield from the internal standard. Coupling constants (*J*) are reported in hertz (Hz).

Reduction of Tri-*n*-butylphosphine oxide—Typical Procedure

Tri-*n*-butylphosphine oxide (448 mg, 2.22 mmol) and a Polytetrafluoroethylene (PTFE)-coated magnetic stir bar were placed in a 10-mL flask; 2 mL of benzene-*d*₆ was added and the solution was cooled down to 5°C. Next, the air was replaced with argon in a usual vacuum degasification sequence. The solution was warmed up to RT and phenylsilane (285 mg, 333 μ L, 2.64 mmol) was added. The flask was sealed with a glass stopper secured by a metal clamp and placed in a 100°C hot oil bath on a hot plate magnetic stirrer for 6 h. After that time, the reaction mixture was cooled down to RT and a sample was carefully taken to record NMR spectra, which indicate the full conversion of the substrate. The pure product was isolated by distillation under reduced pressure to yield 348 mg (72%) of tri-*n*-butylphosphine. The ¹H and ³¹P NMR spectra are consistent with the literature [42, 43], bp 36–38°C/0.2 mmHg (lit.: [44] 38–40°C, 0.2 mmHg).

³¹P NMR (202 MHz, CDCl₃) : δ = -32 ppm;

^1H NMR (500 MHz, CDCl_3): $\delta = 0.8 - 1.0$ (m, 9H),
1.3 – 1.5 (m, 18H);

^{13}C (dept) NMR (125 MHz, CDCl_3): $\delta = 13.8, 24.5$
(d, $J = 11.1$ Hz), 26.9 (d, $J = 10.5$ Hz),
28.1 (d, $J = 12.3$ Hz).

Kinetic Measurements

The starting reaction mixtures were prepared by introducing weighed quantities of tri-*n*-butylphosphine oxide and phenylsilane into an argonated NMR tube. The initial amount of tri-*n*-butylphosphine oxide was 10.6 mg (0.05 mmol), whereas phenylsilane was used in an 80-fold molar excess (500 μL , 4.0 mmol), when the reaction was run without solvent addition, or in a 20-fold molar excess (120 μL), when the reaction was run in a solution in 380 μL of the chosen solvent. The NMR tube was sealed and placed in a preheated oil bath at constant temperatures. The reaction mixtures were analyzed by NMR using TMS (^1H NMR) and capillaries with H_3PO_4 in D_2O (^{31}P NMR) as internal standards. The conversion of phosphine oxide was determined from ^{31}P NMR spectroscopy in 30-min periods (the NMR tube was rapidly chilled before each measurement). We also checked whether the ratio of $\text{Bu}_3\text{PO}/\text{Bu}_3\text{P}$ remained constant during the measurements. To this end, the measured sample was left at RT for 16 h and the ^{31}P NMR spectrum was recorded again—the data analysis revealed no reaction progress between the two measurements. The pseudo-first-order rate constants k' were followed by measuring the area of the NMR peak of Bu_3P (–32 ppm) and Bu_3PO (43 ppm). The kinetic runs were carried out at all temperatures with more than 80% completion of the reactions. The second-order rate constants k were obtained from the quotient of pseudo-first-order rate constants k' and the initial concentration of phenylsilane according to the standard procedure [40].

Quantumchemical Calculations

The quantum-chemical calculations were performed on a SGI-Altix-3700 computer in the Cracow Computing Center “CYFRONET.” Hybrid B3LYP as well as M062x functionals and 6–31G(d), 6–31+G(d), 6–31+G(d,p) basis sets included within GAUSSIAN 2009 software [36] were applied. For the calculations of the solvent effect on the reaction paths, a PCM, in which a cavity is created via a series of overlapping

spheres, was used. DFT (PCM) calculations were performed for vacuum/isolated molecules and for the simulated presence of toluene, which is parameterized by the Gaussian package, and the polarity is relatively close to the polarity of phenylsilane.

The reactivity indexes were estimated according to the equations and theoretical level recommended by Parr and Yang [45] and Domingo and co-authors [31]. In particular, the electronic chemical potentials (μ) and chemical hardness (η) of reactants **1** and **2** were evaluated in terms of one-electron energies of FMO:

$$\mu = (E_{\text{HOMO}} + E_{\text{LUMO}})/2; \eta = E_{\text{LUMO}} - E_{\text{HOMO}}$$

The values of μ and η were then used for calculation of the global electrophilicity (ω) according to the formula:

$$\omega = \mu^2/2\eta$$

The maximum amount of electronic charge that the electrophile system may accept was calculated by the following formula [46]:

$$\Delta N_{\text{max}} = -(\mu/\eta)$$

Optimizations of the stable structures were performed with the Berny algorithm, whereas the transition states were calculated using the QST2 procedure followed by the TS method. Stationary points were characterized by frequency calculations. All reactants, products, and local minima had positive Hessian matrices. All transition states showed only one negative eigenvalue in their diagonalized Hessian matrices, and their associated eigenvectors were confirmed to correspond to the motion along the reaction coordinate under consideration. IRC calculations were performed to connect previously computed transition structures with suitable minima.

ACKNOWLEDGMENTS

The generous allocation of computing time by the regional computer center “Cyfronet” in Cracow (Grant No.: MNiSW/Zeus_lokalnie/PK/009/2013) and support from the Polish National Science Centre (NCN grants number 2012/05/B/ST5/00362) as well as kind aid of Prof. D. Gryko (ICHO PAN, Warsaw) are gratefully acknowledged.

REFERENCES

- [1] Corbridge, D. E. C. Phosphorus: Chemistry, Biochemistry and Technology, 6th ed.; Taylor & Francis: Boca Raton, FL, 2013.
- [2] Keglevich, G.; Kovács, T. *Curr Green Chem* 2014, 1, 182–188, and references cited there.

- [3] Naumann, K.; Zon, G.; Mislow, K. *J Am Chem Soc* 1969, 91, 7012–7023.
- [4] Horner, L.; Balzer, W. D. *Tetrahedron Lett* 1965, 6, 1157–1162.
- [5] Wu, H. C.; Yu, J. Q.; Spencer, J. B. *Org Lett* 2004, 6, 4675–4678.
- [6] Demchuk, O. M.; Yoruk, B.; Blackburn, T.; Snieckus, V. *Synlett* 2006, 2908–2913.
- [7] Berk, S. C.; Buchwald, S. L. *J Org Chem* 1992, 57, 3751–3753.
- [8] Allen, A.; Ma, L.; Lin, W. B. *Tetrahedron Lett* 2002, 43, 3707–3710.
- [9] Yin, J. J.; Buchwald, S. L. *J Am Chem Soc* 2000, 122, 12051–12052.
- [10] Lawrence, N. J.; Drew, M. D.; Bushell, S. M. *J Chem Soc, Perkin Trans 1* 1999, 3381–3391.
- [11] Li, Y. H.; Das, S.; Zhou, S. L.; Junge, K.; Beller, M. *J Am Chem Soc* 2012, 134, 9727–9732.
- [12] Li, Y. H.; Lu, L. Q.; Das, S.; Pisiewicz, S.; Junge, K.; Beller, M. *J Am Chem Soc* 2012, 134, 18325–18329.
- [13] Marsi, K. L. *J Org Chem* 1974, 39, 265–267.
- [14] Pakulski, Z.; Koprowski, M.; Pietrusiewicz, K. M. *Tetrahedron* 2003, 59, 8219–8226.
- [15] Horner, L.; Hoffmann, H.; Beck, P. *Chem Ber-Recl* 1958, 91, 1583–1588.
- [16] Tang, R.; Mislow, K. *J Am Chem Soc* 1969, 91, 5644.
- [17] Imamoto, T.; Kikuchi, S.; Miura, T.; Wada, Y. *Org Lett* 2001, 3, 87–90.
- [18] Griffin, S.; Heath, L.; Wyatt, P. *Tetrahedron Lett* 1998, 39, 4405–4406.
- [19] Bootle-Wilbraham, A.; Head, S.; Longstaff, J.; Wyatt, P. *Tetrahedron Lett* 1999, 40, 5267–5270.
- [20] Busacca, C. A.; Lorenz, J. C.; Grinberg, N.; Haddad, N.; Hrapchak, M.; Latli, B.; Lee, H.; Sabila, P.; Saha, A.; Sarvestani, M.; Shen, S.; Varsolona, R.; Wei, X. D.; Senanayake, C. H. *Org Lett* 2005, 7, 4277–4280.
- [21] Zablocka, M.; Delest, B.; Igau, A.; Skowronska, A.; Majoral, J. P. *Tetrahedron Lett* 1997, 38, 5997–6000.
- [22] O'Brien, C. J.; Lavigne, F.; Coyle, E. E.; Holohan, A. J.; Doonan, B. J. *Chem-Eur J* 2013, 19, 5854–5858.
- [23] O'Brien, C. J.; Nixon, Z. S.; Holohan, A. J.; Kunkel, S. R.; Tellez, J. L.; Doonan, B. J.; Coyle, E. E.; Lavigne, F.; Kang, L. J.; Przeworski, K. C. *Chem-Eur J* 2013, 19, 15281–15289.
- [24] O'Brien, C. J.; Tellez, J. L.; Nixon, Z. S.; Kang, L. J.; Carter, A. L.; Kunkel, S. R.; Przeworski, K. C.; Chass, G. A. *Angew Chem, Int Ed* 2009, 48, 6836–6839.
- [25] van Kalker, H. A.; Leenders, S. H. A. M.; Hommersom, C. R. A.; Rutjes, F. P. J. T.; van Delft, F. L. *Chem-Eur J* 2011, 17, 11290–11295.
- [26] O'Brien, C. J. *US Patent* 20120029211, 2012.
- [27] O'Brien, C. J.; Patent WO/2010/118042, 2010.
- [28] (a) Zhao, W.; Yan, P. K.; Radosevich, A. T. *J Am Chem Soc* 2015, 137, 616–619; (b) Hirose, D.; Taniguchi, T.; Ishibashi, H. *Angew Chem, Int Ed* 2013, 52, 4613–4617.
- [29] Dunn, P. J.; Hii, K. K.; Krische, M. J.; Williams, M. T. *Sustainable Catalysis: Challenges and Practices for the Pharmaceutical and Fine Chemical Industries*; Wiley: Hoboken, New Jersey, 2013.
- [30] Krenske, E. H. *J Org Chem* 2012, 77, 3969–3977.
- [31] Perez, P.; Domingo, L. R.; Aizman, A.; Contreras, R. *Theoretical Aspects of Chemical Reactivity*; Elsevier: Amsterdam, the Netherlands, 2007.
- [32] Chattaraj, P. K.; Giri, S.; Duley, S. *Chem Rev* 2011, 111, Pr43–Pr75.
- [33] Jasinski, R. *Curr Chem Lett* 2013, 1, 157–162.
- [34] Kapłon, K.; Demchuk, O. M.; Wieczorek, M.; Pietrusiewicz, K. M. *Curr Chem Lett* 2014, 3, 23–36.
- [35] Meneses, L.; Araya, A.; Pilaquinga, F.; Fuentealba, P. *Chem Phys Lett* 2008, 460, 27–30.
- [36] Frisch, M. J.; Trucks, G. W.; Schlegel, H. B.; Scuseria, G. E.; Robb, M. A.; Cheeseman, J. R.; Scalmani, G.; Barone, V.; Mennucci, B.; Petersson, G. A.; Nakatsuji, H.; Caricato, M.; Li, X.; Hratchian, H. P.; Izmaylov, A. F.; Bloino, J.; Zheng, G.; Sonnenberg, J. L.; Hada, M.; Ehara, M.; Toyota, K.; Fukuda, R.; Hasegawa, J.; Ishida, M.; Nakajima, T.; Honda, Y.; Kitao, O.; Nakai, H.; Vreven, T.; Montgomery, J. A., Jr.; Peralta, J. E.; Ogliaro, F.; Bearpark, M.; Heyd, J. J.; Brothers, E.; Kudin, K. N.; Staroverov, V. N.; Kobayashi, R.; Normand, J.; Raghavachari, K.; Rendell, A.; Burant, J. C.; Iyengar, S. S.; Tomasi, J.; Cossi, M.; Rega, N.; Millam, N. J.; Klene, M.; Knox, J. E.; Cross, J. B.; Bakken, V.; Adamo, C.; Jaramillo, J.; Gomperts, R.; Stratmann, R. E.; Yazyev, O.; Austin, A. J.; Cammi, R.; Pomelli, C.; Ochterski, J. W.; Martin, R. L.; Morokuma, K.; Zakrzewski, V. G.; Voth, G. A.; Salvador, P.; Dannenberg, J. J.; Dapprich, S.; Daniels, A. D.; Farkas, O.; Foresman, J. B.; Ortiz, J. V.; Cioslowski, J.; Fox, D. J., *Gaussian'09, Revision A.1*; Gaussian: Wallingford, CT, 2009.
- [37] (a) Camps, P.; Colet, G.; Segura, S.; Vazquez, S. *Arkivoc* 2007, 8–19; (b) Prezhdo, O. V.; Gawdzik, B.; Zubkova, V. V.; Prezhdo, V. V. *J Mol Struct* 2009, 919, 146–153.
- [38] Zhao, Y.; Truhlar, D. G. *Theor Chem Acc* 2008, 120, 215–241.
- [39] (a) Diallo, O. S.; Brazier, J.-F.; Kläbe, A.; Wolf, R. *Phosph Sulf Silicon* 1985, 22, 93–97; (b) Tangour, B.; Malavalid, C.; Boisdon, M. T.; Barrans, J. *Phosph Sulf Silicon* 1988, 40, 33–39; (c) Fliss, O.; Bessrou, R.; Tangour, B. *J Mol Struct Theorchem* 2006, 758, 225–232.
- [40] Schwetlick, K. *Kinetische Methoden zur Untersuchung von Reaktionsmechanismen*; Deutscher Verlag der Wissenschaften: Berlin, Germany, 1971.
- [41] Coyle, E. E.; Doonan, B. J.; Holohan, A. J.; Walsh, K. A.; Lavigne, F.; Krenske, E. H.; O'Brien, C. J. *Angew Chem, Int Ed* 2014, 126, 13121–13125.
- [42] Sigma-Aldrich FTNMR, T49484. Available at http://www.sigmaaldrich.com/spectra/fnmr/FNMR_011481.PDF.
- [43] Nifant'ev, E. E.; Vasyanina, L. K.; *Spektroskopiya YMR P-31*; Moskovski Gosudarstvennyi Pedagogicheski Institut: Moscow, Russia, 1986.
- [44] Omelanczuk, J.; Mikolajczyk, M. *J Am Chem Soc* 1979, 101, 7292–7295.
- [45] Parr, R. G.; Yang, W. *Density-Functional Theory of Atoms and Molecules*; Oxford University Press/Clarendon Press: New York / Oxford, UK, 1989.
- [46] Perez, P.; Domingo, L. R.; Aurell, A. J.; Contreras, R. *Tetrahedron* 2003, 59, 3117–3125.